Cellulose (2011) 18:957–973
DOI 10.1007/s10570-011-9543-x

Poly(oxyethylene) and ramie whiskers based nanocomposites: influence of processing: extrusion and casting/evaporation

Fannie Alloin · Alessandra D'Aprea · Alain Dufresne · Nadia El Kissi · Frédéric Bossard

Received: 21 May 2010 / Accepted: 5 April 2011 / Published online: 20 April 2011

Abstract Polymer nanocomposites were prepared from poly(oxyethylene) PEO as the matrix and high aspect ratio cellulose whiskers as the reinforcing phase. Nanocomposite films were obtained either by extrusion or by casting/evaporation process. Resulting films were characterized using microscopies, differential scanning calorimetry, thermogravimetry and mechanical and rheological analyses. A thermal stabilization of the modulus of the cast/evaporated nanocomposite films for temperatures higher than the PEO melting temperature was reported. This behavior was ascribed to the formation of a rigid cellulosic network within the matrix. The rheological characterization showed that nanocomposite films have the typical behavior of solid materials. For extruded films, the reinforcing effect of whiskers is dramatically reduced, suggesting the absence of a strong mechanical network or at least, the presence of a weak whiskers percolating network. Rheological, mechanical and microscopy studies were involved in order to explain this behavior.

Keywords Polymer matrix composites · Cellulose whiskers · Thermal properties · Dynamic mechanical analysis · Rheology · Extrusion

A. D'Aprea · N. E. Kissi · F. Bossard
Laboratoire de Rhéologie, UMR 5520, Grenoble-INP-CNRS-UJF, BP 53, 38041 Grenoble Cedex 9, France

F. Alloin (✉) · A. D'Aprea
LEPMI, Laboratoire d'Electrochimie et de Physicochimie des Matériaux et des Interfaces, UMR 5279, CNRS-Grenoble INP-Université de Savoie - Université Joseph Fourier, BP 75, 38402 Grenoble Cedex 9, France
e-mail: fannie.alloin@lepmi.grenoble-inp.fr

A. D'Aprea · A. Dufresne
The International School of Paper, Print Media and Biomaterials (Pagora), Grenoble-INP, BP 65, 38402 Saint Martin d'Hères Cedex, France

Introduction

During the last decade, natural fibers reinforced thermoplastic polymers have attracted the attention of both the academic and industrial world for applications in transport and construction. This considerable interest in the possibility of replacing conventional fibers, like glass fibers, is ascribed to well-known advantages such as renewable nature, low cost and density. However, one of the main drawbacks of lignocellulosic fibers is the big variation of properties inherent to any natural products. Their properties are related to climatic conditions, maturity, and type of soil. Disturbances during plant growth also affect the plant structure and are responsible for the enormous disparity of mechanical plant fiber properties. One of the basic idea to achieve further improved fiber and composite is to eliminate the macroscopic flaws by destructuring the natural grown fibers, and separating the almost defect free highly crystalline fibrils. When combining this process with an acidic treatment, high

specific surface area rod-like nanoparticles of monocrystalline cellulosic fragments can be obtained. The state of dispersion of these nanoparticles, called cellulose whiskers, in a polymeric matrix has an important impact on the final properties of composites and is strongly dependent on the processing technique and conditions.

In a previous study (Azizi Samir et al. 2004a), poly(oxyethylene) (PEO) films have been reinforced with tunicin whiskers. PEO being a hydrosoluble polymer and cellulose whiskers being obtained as aqueous suspensions, the processing of nanocomposite films was easily carried out by mixing the two constituents in water and casting the resultant dispersion. The important aspect ratio of tunicin whiskers make these cellulose nanoparticles derived from tunicate, a sea animal, a good candidate for modeling rheological and reinforcement behaviors and it was extensively studied in the literature (Favier et al. 1995). However, this source of cellulose is not suitable for technical applications due to its poor availability. Such rod-like nanoparticles with various aspect ratios can also be extracted from other renewable resources as plant fibers (Azizi Samir et al. 2005a). In the present study, cellulose whiskers were extracted from ramie fibers.

Very few studies have been reported concerning the processing of cellulose whiskers reinforced nanocomposites by extrusion methods. An attempt to prepare nanocomposites based on cellulose whiskers obtained from microcrystalline cellulose and poly(lactic acid), PLA, by melt extrusion technique was recently reported (Oksman et al. 2006; Bondeson and Oksman 2007). The suspension of nanocrystals was pumped into the polymer melt during the extrusion process. Organic acid chlorides-grafted cellulose whiskers were also extruded with low density polyethylene (De Menezes et al. 2009).

In the present study, we investigate the preparation and the properties of nanocomposite films obtained from PEO as the matrix and cellulose whiskers extracted from ramie as the reinforcing phase. Both casting/evaporation, largely employed in research, and extrusion processing method, a more industrial technique, have been used. Thermogravimetric analysis (TGA) and differential scanning calorimetry (DSC) measurements have been used to investigate the thermal characteristics and degradation of the ensuing nanocomposites. The viscoelastic behavior of these materials was investigated in both the molten and solid states as a function of the whiskers content and processing technique by rheological and mechanical methods. In the first part of the paper, the effect of the ramie whiskers content on the properties for cast/evaporated nanocomposite films was investigated. In the second part, the impact of the processing technique was examined, restricting the study to a film reinforced with 6 wt% ramie whiskers.

Experimental methods

Nanocomposite films

Materials

Poly(oxyethylene), PEO, with a high molecular weight ($M_w = 5 \times 10^6$ g mol^{-1}) was purchased as a white powder from Aldrich and used as received.

Cellulose whiskers were prepared from ramie fibers as described in details elsewhere (Habibi and Dufresne 2008). Briefly, ramie fibers were cut into small pieces and treated with 2 wt% NaOH at 80 °C for 2 h to remove residual additives. The purified ramie fibers were submitted to acid hydrolysis with a 65 wt% H_2SO_4 solution at 55 °C for 30 min and under continuous stirring. The suspension was washed with water by centrifugation and dialyzed to neutrality against deionized water. The obtained suspension was homogenized using an Ultra Turrax T25 homogenizer for 5 min at 13,500 rpm and then filtered in sintered glass No. 1 to remove unhydrolyzed fibers. The suspension was concentrated to constitute the stock suspension. This treatment leads to aqueous suspensions of high aspect ratio rod-like nanocrystals, characterized by an average dimension of the cross section d of 6–8 nm and a length L ranging between 150 and 250 nm, measured by TEM (Habibi et al. 2007; Habibi and Dufresne 2008). The average aspect ratio L/d and the specific surface area of these whiskers were estimated to be close to 28 ± 12 and 380 ± 38 m^2 g^{-1}, respectively, taking 1.5 g cm^{-3} for the density of cellulose.

Processing of nanocomposite films

Cast/evaporated films The desired amount of ramie whiskers aqueous suspension was added to the PEO, previously dispersed in a few milliliter of methanol

for a better dissolution. The cellulose whiskers content was varied from 0 to 30 wt% (dry basis). The resulting suspension was protected against light by an aluminum foil and was weakly stirred for 4 days at room temperature. The suspension was then degassed under vacuum in order to remove the remaining air, cast into Teflon plates and dried under argon at 40 °C for 3 weeks. The films were then progressively dried under vacuum for a week with a temperature increase step of 5 °C per day from 40 to 75 °C and finally stored in glove box. The thickness of final films was about 200–300 μm.

Extruded films Poly(oxyethylene) matrix and ramie whiskers reinforced PEO nanocomposite films were prepared by extrusion. First, the PEO solution and cellulose whiskers/PEO suspensions with 6 wt% ramie whiskers were prepared similarly to the previous description. The suspension was degassed under vacuum and the water was removed by freeze-drying. The ensuing powder was introduced in the mixing chamber of a twin-screw DSM Micro 15 compounder and allowed to melt under nitrogen flow at 180 °C. The mixing speed was set at 25 rpm for 10 min. Extrusion was carried out with a slit die of 0.6 mm in gap and 1 cm in length. The extruded films were then cooled and calendered. They were homogeneous, smooth, and bubble-free. The film thickness ranged between 400 and 500 μm. The films were dried for 4 days at 75 °C under vacuum and then stored in glove box.

Characterizations

Microscopies

Scanning electron microscopy (SEM) was used to investigate the morphology of the nanocomposite films using a LEO S440 SEM instrument. The samples were frozen under liquid nitrogen, fractured, mounted, coated with graphite and observed using an accelerating voltage of 10 kV.

Transmission electron microscopy (TEM) observations were made with a Philips CM200 electron microscope. A droplet of a dilute suspension of re-dispersed extruded nanocomposite films with 6 wt% of cellulose whiskers was deposited and dried on a carbon coated grid with one droplet ($\sim$6 μl) of uranyl acetate solution (2 wt%) to carry out the negative coloration which emphasizes cellulose. The accelerating voltage was 80 kV.

A ZEISS polarizing optical microscope was used to observe and follow the growth of the PEO spherulites. The microscope was connected to a LINKAM 20 to control the temperature. Samples were melted at 100 °C for few minutes and then cooled to the crystallization temperature. Average radius values of spherulites were measured assuming a circular shape.

Differential scanning calorimetry

Differential scanning calorimetry tests were performed using a TA Instrument DSC, DSC2920 CE. Standard modes were performed. Samples of 10 mg were sealed in aluminum pans and placed in the DSC cell in glove box. Each sample was heated from −100 to 100 °C at a temperature ramp of 10 °C min^{-1} and kept at this temperature for 5 min to insure the thermal equilibrium. Then, it was cooled down to 0 °C at a temperature ramp of 10 °C min^{-1}. The melting temperature, T_m, and the crystallization temperature, T_c, were taken at the onset of the melting and crystallization peaks, respectively.

Thermogravimetric analysis

Thermogravimetric analysis measurements were carried out with a Netzsch STA409 thermal analyzer. Around 10 mg of the sample were heated from room temperature up to 550 °C at 10 °C min^{-1} under either air or nitrogen flow. The results allow following the weight loss as a function of the temperature. The degradation temperature was associated with the beginning of the weight loss.

Dynamic mechanical analysis

Dynamic mechanical analysis (DMA) measurements were carried out with a spectrometer DMA Q800 from TA Instrument working in the tensile mode. The strain amplitude was fixed at 0.05%, well below the limit of the linear viscoelastic regime. The samples were thin rectangular strips with dimensions of about $20 \times 7 \times 0.2$ mm^3 for cast/evaporated films and $20 \times 7 \times 0.4$ mm^3 for extruded films. Measurement of the storage tensile modulus, E', was performed in isochronal condition (1 Hz), and the temperature was

varied between −100 and 150 °C using a temperature ramp of 2 °C min^{-1}.

Rheometry measurements

Rheometrical data were collected with a rotating ARG2 rheometer from TA Instrument operating under controlled strain conditions. It was equipped with an oven and the analysis was carried out up to 180 °C under nitrogen flow. The storage shear modulus G' and the loss shear modulus G'' of the samples were measured in the linear viscoelastic regime using a parallel plates geometry of 25 mm in diameter, with a gap of 500 μm. The dynamic viscosity was calculated from G' and G'' moduli.

Creep measurements for cast/evaporated and extruded nanocomposites were performed on the sample at 90 °C and at the same stress, corresponding to a torque of 5 μNm.

Results and discussions

Cast/evaporated films

Morphology

The PEO films reinforced with ramie whiskers were characterized by scanning electron microscopy (SEM). Figure 1 shows the cryofractured surface for the cast/evaporated unfilled PEO matrix and nanocomposite film filled with 6 wt% ramie whiskers. The surface of the cast/evaporated PEO matrix (Fig. 1a) appears homogeneous without voids. The cryofractured surface of the cast/evaporated nanocomposite film is more chaotic than the matrix and shows a homogeneous dispersion of white dots (Fig. 1b). The cross sections of these dots do not correspond to the one of isolated whiskers, since their dimensions are far higher than those of the whiskers. Indeed, it was shown that the white dots result from electrical charge effects that increase the apparent cross section of whiskers (Anglés and Dufresne 2000).

Thermal characterization

The melting process was studied during the first heating scan. For unfilled specimens, measurements were performed for PEO powder and for the neat cast/evaporated PEO matrix. No significant difference was reported between both unfilled materials as can be seen in Table 1.

Melting temperature The melting temperature, T_m, remains roughly constant for low whisker content, up to 6 wt% (Table 1). At high filler content, i.e. 20 and 30 wt%, a weak decrease in T_m is observed. This behavior is in good agreement with that reported by (Azizi Samir et al. 2004a) for tunicin whiskers and (Guo and Liang 1999) for wheat straw cellulose whiskers. The decrease of the melting temperature may be associated to the decrease of the spherulite size. Indeed, a large decrease of the spherulite size was observed with the incorporation of tunicate whiskers in PEO matrix (Azizi Samir et al. 2005b).

Degree of crystallinity The degree of crystallinity of the PEO matrix, χ_m, was calculated using the ratio

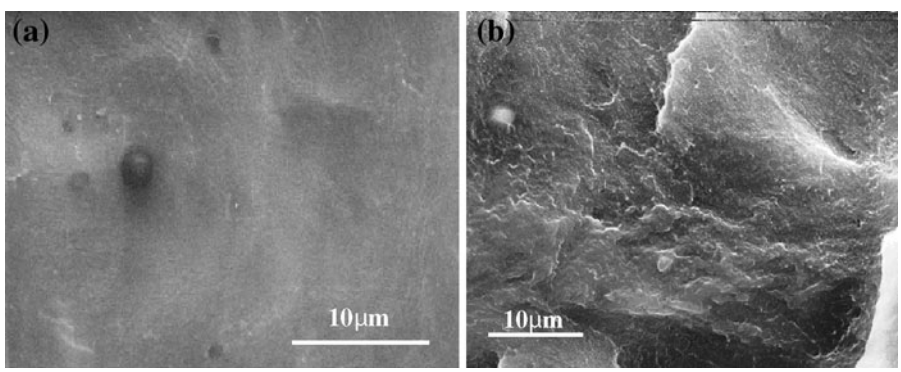

Fig. 1 Scanning electron micrographs of the cryofractured surface for the cast/evaporated **a** PEO film and **b** PEO film reinforced with 6 wt% of ramie whiskers

Table 1 Thermal characteristics of cast/evaporated PEO-based nanocomposites reinforced with ramie whiskers obtained from DSC and ATG curves: crystallization temperature (T_c), melting temperature (T_m), degree of crystallinity expressed as a function of the matrix weight measured during the melting (χ_m), degradation temperature (T_{onset}), activation energies

Samples	T_c (°C)	T_m (°C)	χ_m^a	T_{onset} (10 °C min^{-1})$_{Air}$	T_{onset} (10 °C min^{-1})$_{He}$	E_a (kJ mol^{-1})
Ramie W.	–	–	–	270	265	–
PEO powder	51	57	0.82	–	350	380
PEO	51	56	0.81	205	–	–
PEO + 3 wt% WR	50	56	0.82	194	352	205
PEO + 6 wt% WR	50	57	0.80	191	357	210
PEO + 10 wt% WR	47	56	0.80	188	345	190
PEO + 20 wt% WR	46	53	0.76	187	320	170
PEO + 30 wt% WR	45	53	0.75	185	310	180

[a] $\chi_m = \frac{\Delta H_{m-PEO}}{\Delta H_m^0}$ where $\Delta H_m^0 = 210$ J g^{-1} is the heat of melting for 100% crystalline PEO

between the melting enthalpy determined by DSC and the one corresponding to 100% crystalline PEO. It was calculated per gram of PEO to take into account the presence of the filler. The effect of the whiskers content on the degree of crystallinity of PEO is weak and it is only observed for highly filled specimens for which a slight decrease of the degree of crystallinity is observed upon ramie whiskers addition.

Degradation behavior

The thermal stability of ramie whiskers reinforced PEO nanocomposites was characterized using thermogravimetric analysis. In these experiments, the weight loss of cast/evaporated nanocomposite films was plotted in Fig. 2 as a function of temperature under air flow with a temperature ramp of 10 °C min^{-1}.

PEO matrix and whiskers degradations

The onset degradation temperature, i.e. the temperature associated with the beginning of the weight loss, was found to be 205 °C for the unfilled PEO matrix (Table 1). The PEO degradation under oxygen atmosphere induces the formation of a large number of volatile products involving several mechanisms (Costa et al. 1992).

The thermo-oxidative degradation of pure ramie whiskers was also investigated and the degradation temperature was found to be 270 °C (Table 1; Fig. 2). The degradation of ramie whiskers occurs

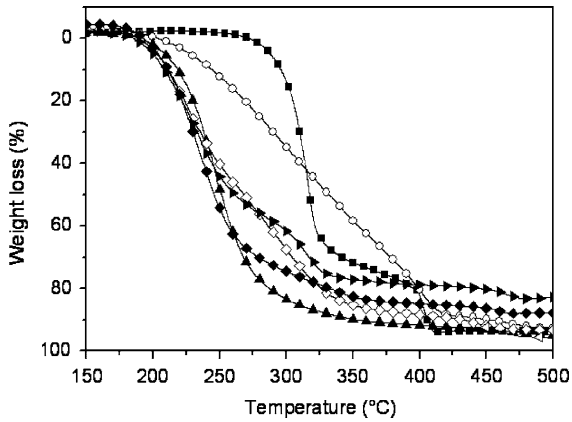

Fig. 2 Weight loss of unfilled PEO matrix (*open circle*), ramie whiskers (*filled square*) and related nanocomposite films reinforced with 3 (*filled triangle*), 6 (*inverted triangle*), 10 (*diamond*), 20 (*open triangle*) and 30 wt% (*right-pointing triangle*) of ramie whiskers versus temperature. Measurements were performed under continuous flow of dry air

following two steps. The first one at low temperature may correspond to the cellulose depolymerization induced by the glucosidic bond scission which involves hemicellulose formation, and the second step, at about 400 °C, is most probably associated with the thermal degradation of the α-cellulose, by similarity with the degradation process reported for sisal fibers (Alvarez et al. 2004).

Composite degradation under air flow

The weight loss observed for filled PEO films starts at lower temperature compared to neat PEO, from 194 to 185 °C for the composites and at 205 °C for neat

PEO (Table 1; Fig. 2). A significant decrease of the onset degradation temperature of the filled matrix is observed even at low whisker content. It is roughly 25–30 °C lower than the onset degradation temperature of the neat polymer. Furthermore, the weight loss kinetic is notably enhanced in the presence of ramie whiskers (Fig. 2). Indeed, the quasi-total degradation of the filled samples is observed at 300 °C, whereas it is achieved at 400 °C in the case of neat PEO.

These results indicate a large effect of the presence of whiskers on the PEO thermal stability even if the whisker degradation occurs at high temperature.

(Chauvin et al. 2006) have shown that PEO is very sensitive to acid medium and a strong decrease of its molecular weight was observed. Furthermore, a net decrease of the thermal stability of oligoether sulfate (Chauvin et al. 2005) was observed in the presence of a small amount of water, indicating the sensibility of PEO degradation to the presence of both water and sulfate acidic function. Thus, the sulfate ester groups present at the whisker surface and resulting from the acid hydrolysis treatment with sulfuric acid can have a strong influence on the filled PEO degradation.

At low acid concentration, the sulfate ester groups induce a significant decrease of the cellulose thermal stability under air flow (Roman and Winter 2004; Kim et al. 2001; Julien et al. 1993; Parks 1971; Tang and Neill 1964). During the first degradation step starting at 150 °C, the desulfation and dehydration of the cellulose occur (Guo and Liang 1999). The latter effect increases the water content in the medium and catalyzes the degradation reaction of cellulose (Scheirs et al. 2001).

Effect of acidic surface density

In order to evaluate the influence of sulfate acid groups, present at the whisker surface, on the thermal degradation of PEO based composites, the surface density of sulfate groups of the ramie whiskers was determined by titration using NaOH solution. It was equal to 0.022 e/nm^2 ± 0.001, taking 380 m^{2}g^{-1} as the specific surface area of the ramie whiskers. This value is low but appears to be sufficient to induce a decrease of the thermal stability of the cellulosic nanoparticles (Roman and Winter 2004) without a significant weight loss. This degradation induces the formation of sulfate acid and water in the medium, which may enhance the PEO degradation by hydrolysis. Indeed, the ether oxygen could provide hydroxyl groups using acid catalysis, and then the dehydratation of the PEO occurs (Grassie and Mendoza 1985). The degradation of PEO is enhanced by its oxidation induced by the presence of O_2.

The activation energy, E_a, of this degradation process can be determined using the Broido's method (Broido 1969) as follows:

$$\ln\left(\ln\frac{1}{y}\right) = -\frac{E_a}{R}\frac{1}{T} + C \quad (1)$$

where y is the fraction of degraded product at time t, R, T and C are the gas constant, the temperature and a temperature independent term, respectively. E_a/R is given by the slope of the plot of ln (ln $1/y$) as a function of $1/T$. The activation energy obtained for filled PEO is much lower than that obtained for neat PEO (Table 1). This result suggests that the degradation reaction is initiated by the whiskers degradation. The PEO degradation is then catalyzed by the sulfuric acid and water present in the medium.

In order to reduce the influence of sulfate acid groups brought by the cellulose whiskers on the thermal degradation of filled PEO, the whisker suspension was neutralized by NaOH solution. A nanocomposite film reinforced with 6 wt% of ramie whiskers was prepared using these neutralized whiskers. TGA results are reported in Fig. 3. The onset degradation temperature is similar for nanocomposite

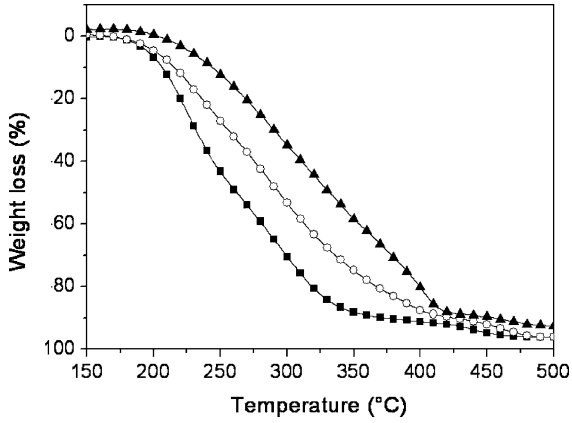

Fig. 3 Weight loss of the unfilled PEO matrix (*filled triangle*), and related composites reinforced with 6 wt% of untreated ramie whiskers (*filled square*) and neutralized ramie whiskers (*open circle*) versus temperature. Measurements were performed under continuous dry air flow

films reinforced with neutralized or untreated whiskers (Fig. 3). However, the degradation kinetic observed with neutralized whiskers based composite is lower than that obtained with untreated whiskers based composite.

The degradation activation energy of the nanocomposite film reinforced with 6 wt% neutralized whiskers is about 217 kJ mol^{-1} which is notably higher than the value obtained for the nanocomposite film reinforced with untreated whiskers (190 kJ/mol^{-1}) but lower than the value obtained for neat PEO (380 kJ/mol^{-1}). The influence of acidic functions at the surface of the whiskers towards the degradation of the PEO matrix is clearly evidenced; however the addition of neutral whiskers has also a negative impact on the PEO matrix thermal stability. During the whiskers neutralization, the acid function is transformed in a sodium salt. It has been reported that alkaline salts have an influence on the degradation of PEO (Costa et al. 1992). The strong interaction between the cation and the ether oxygen involves the weakening of the C–O bond and favors its scission under air flow. In filled PEO, such interactions may occur in addition to hydrogen bonding between cellulose OH groups and PEO. These interactions may explain the decrease in thermal stability observed in comparison to the neat PEO.

Composite degradation under helium flow

The study of the thermal degradation of ramie whiskers reinforced PEO films was carried out under inert atmosphere, i.e. helium, to avoid any oxidizing character of the medium. Results are reported in Table 1. The onset degradation temperature of PEO films, initially at about 205 °C in the presence of air is shifted to 350 °C under helium, showing the dominating effect of oxygen in the PEO degradation mechanism (Cameron et al. 1989), whereas no shift of the degradation temperature was reported for ramie whiskers.

Compared to the neat PEO, the presence of a low amount of cellulose whiskers does not modify the thermal stability of composites. For filled films, the degradation process under helium occurs in two distinct steps, starting by the cellulose and followed by that of PEO (this two steps process is clearly observed for the PEO + 30 wt% WR). The same degradation behavior, involving a two steps process, was reported for a poly(propylene) matrix filled with sisal microfibrils (Panaitescu et al. 2008).

Mechanical behavior

The temperature dependence of the storage tensile modulus E' for the unfilled cast/evaporated PEO matrix and related composites is shown in Fig. 4. In order to minimize the effect of the sample dimension uncertainty on the accuracy of the measurement, the glassy modulus, E' at −100 °C, was normalized at 8.5 GPa for all the samples. It corresponds to the observed average value regardless the composition of the film. The unfilled PEO displays a typical behavior of semi-crystalline polymer.

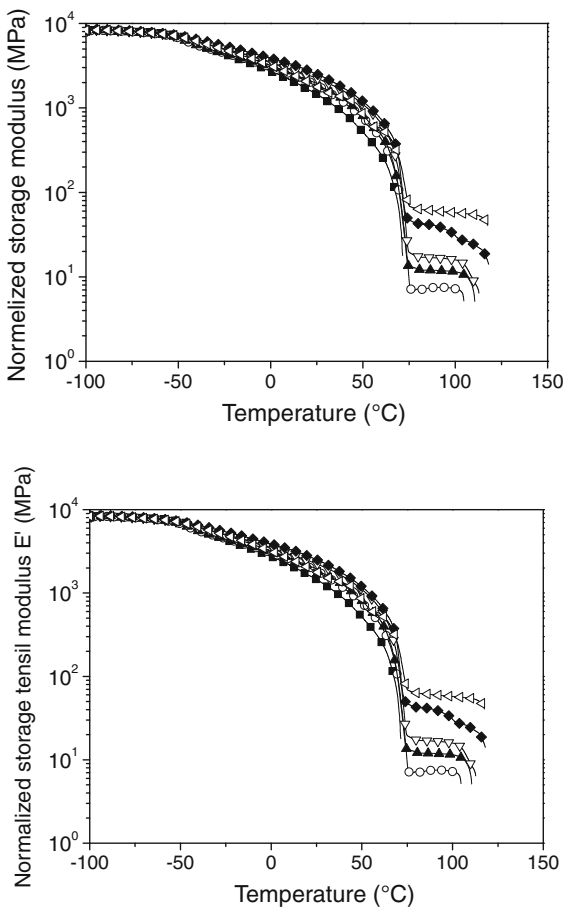

Fig. 4 Normalized storage tensile modulus E' for cast/evaporated unfilled PEO (*filled square*) and nanocomposite films reinforced with 3 (*open circle*), 6 (*filled triangle*), 10 (*inverted triangle*), 20 (*diamond*) and 30 wt% (*left-pointing triangle*) of ramie whiskers as a function of temperature

The relaxation associated with the glass transition of the amorphous domains of PEO occurs at about −55 °C. The modulus drop corresponding to this relaxation is weak because of the high degree of crystallinity of PEO. Above −55 °C, E' decreases continuously because of the progressive softening of PEO. When reaching the melting point of the polymeric matrix around 70 °C, the modulus drops irreversibly for the neat PEO.

When adding ramie whiskers, the rubbery modulus, observed below the PEO melting temperature, slightly increases due to the reinforcing effect of whiskers. Indeed, due to the high crystallinity content of PEO, the rubbery modulus of PEO is very high and was weakly modified by whiskers addition. The main effect is the thermal stabilization of the storage modulus above the melting point of PEO, T_m, up to temperatures higher than 100 °C.

As stressed in Table 2, the value of this high temperature modulus increases as the whiskers content in the nanocomposite film increases. This phenomenon may be ascribed to the formation of a rigid percolating cellulose whiskers network within the polymeric matrix through strong whiskers/whiskers hydrogen bonds interaction (Takayanagi et al. 1964). The modulus of this continuous network can be well predicted from the adaptation of the percolation concept to the classical series–parallel model. In this model and at sufficiently high temperature, i.e. when the storage modulus of the matrix is much lower than that of the percolating network, the following equation was derived (Dufresne et al. 1997) for the predicted elastic modulus, E'_{pre}, of the composite:

$$E'_{pre} = \Psi E'_R \quad \text{With:} \quad \Psi = 0 \quad \text{for} \quad \upsilon_R > \upsilon_{Rc} \tag{2}$$

Table 2 High temperature ($T = 80$ °C) tensile modulus: comparison between experimental (E'_{exp}) and predicted (E'_{pre}) data for ramie whiskers reinforced PEO nanocomposite films

Sample	3 wt%	6 wt%	10 wt%	20 wt%	30 wt%
E'_{exp} (MPa)	8	12	20	40	60
E'_{pre} (MPa)	–	4	9	20	34

With:

$$\Psi = \upsilon_R \left(\frac{\upsilon_R - \upsilon_{Rc}}{1 - \upsilon_{Rc}} \right)^b \quad \text{for} \quad \upsilon_R > \upsilon_{Rc} \tag{3}$$

where Ψ and E'_R are the volume fraction and the elastic modulus of the rigid percolating network, respectively; υ_R, υ_{Rc} and b correspond to the volume fraction of filler, critical volume fraction of filler at the percolation threshold and the corresponding critical exponent, respectively. For a 3D network, $b = 0.4$ (De Gennes 1979) and $\upsilon_{Rc} = 2.5$ vol% was determined from the aspect ratio of ramie whiskers, $L/d = 28$.

The tensile modulus of dry ramie whiskers films, E'_R, was experimentally determined and a value of about 0.35 GPa was found. This value results from the average of two experiments that were relatively reproducible despite the extreme brittleness of the films. This brittleness is no more observed in the PEO/whiskers composite. The low value of the tensile modulus obtained for ramie whiskers, could be associated with the low aspect ratio of ramie whiskers. Indeed, Bras et al. (Bras et al. 2010) shown a correlation between the tensile modulus and the aspect ratio for a large number of whisker sources.

For the predicted modulus, the densities of ramie whiskers and PEO were taken as 1.5 and 1.2 g cm^{-3}, respectively. The predicted storage modulus values, E'_{pre}, are reported in Table 2. They were not determined for the nanocomposite film reinforced with 3 wt% of ramie whiskers, because this filler content is slightly lower than the theoretical percolation threshold value. However, experimentally, a stabilization of the storage tensile modulus was observed with 3 wt% ($\upsilon_{Rc} = 2.41$ vol%) whiskers PEO composite, thus very close to the theoretical percolation threshold. This difference may be associated with the model developed, which neglects the effect of whiskers reinforcement below the percolation threshold.

Regardless the composition of the sample, experimental modulus values, E'_{exp}, display a similar evolution to the predicted one even if experimental values were normalized at low temperature. It is a good indication that the stiffness of the sample and the temperature stabilization of the composite modulus most probably result from the formation of an H-bonded cellulose whiskers network as proposed in the model.

Even if the H-bonded strength decreases with increasing temperature, the large number of H-bonds

involved in whiskers/whiskers interaction induces the stabilization of the composite storage modulus (Favier et al. 1997).

A previous study has shown that for composites based on a PEO matrix and tunicin whiskers, the experimental high temperature modulus values were about 18, 45, and 235 MPa for composites filled with 3, 6, and 10 wt% whiskers, respectively (Azizi Samir et al. 2005b). Compared to ramie whiskers-based nanocomposites, the higher modulus values obtained for tunicin whiskers-based nanocomposites are mainly ascribed to both the higher aspect ratio of tunicin whiskers, of about 70 (only 30 for ramie whiskers) and the higher elastic modulus of the tunicin network.

Impact of film processing

Extrusion is an industrial method allowing to manufacture a large range of products in short times. We investigated the effect of this industrial process on the properties of ramie whiskers reinforced PEO nanocomposite films. The whiskers content was fixed at 6 wt%, i.e. 4.86 vol%. Indeed, this amount is higher than the percolation threshold (2.5 vol%) and corresponds to the optimum balance between a low whiskers content and a strong reinforcing effect.

The processing may have a direct impact on both the thermal and mechanical properties of the composite films because the extrusion process induces mechanical and temperature stresses and some possible orientation of the fibers.

In order to determine the optimized extrusion conditions, the isothermal stability of PEO was investigated by TGA and rheological measurement under inert atmosphere. Neat PEO and PEO reinforced with 6 wt% ramie whiskers samples were maintained at 180 °C for 8 h, and the weight loss observed was only equal to 2% of the initial sample weight and was associated to water evaporation. This result is in accordance with data obtained upon heating in Table 1 and Fig. 2, which show that the onset degradation temperature of PEO was well above 180 °C. The Fig. 5 shows the evolution of both G' and G'' moduli versus time at 180 °C and 1 Hz for the matrix obtained by melting PEO powder. The moduli are constant indicating the stability of PEO at 180 °C in inert atmosphere. The extrusion process was thus performed in a twin screw, under nitrogen flow in order to avoid the oxidation of PEO at

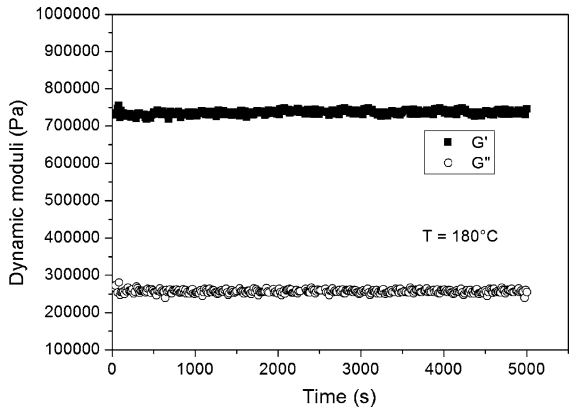

Fig. 5 Storage (G', *filled square*) and loss (G'', *open circle*) moduli versus time at 180 °C for neat PEO, frequency 1 Hz, deformation amplitude 0.5%

180 °C. This temperature seems to be a good compromise between low viscosity and thermal stability. The extrusion speed was maintained at a low value, i.e. 25 rpm, to limit the PEO chains and whiskers break.

Morphology of extruded films

The morphology of the extruded nanocomposite film reinforced with 6 wt% of ramie whiskers was characterized by SEM. Figure 6 shows the cryofractured surface of this material.

The morphology of the extruded nanocomposite film is similar but less chaotic than its cast/evaporated counterpart (Fig. 1b). The extruded film didn't

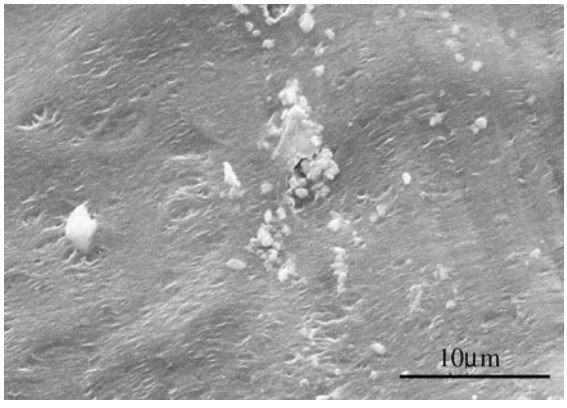

Fig. 6 Scanning electron micrographs of cryofractured surface of the extruded nanocomposite film reinforced with 6 wt% ramie whiskers

display voids but large domains of white dots indicating that the whiskers are not well dispersed in the PEO matrix. The dots observed are much larger than those obtained for the cast/evaporated film, shown in Fig. 1b. The freeze-dried sample, before extrusion, does not exhibit such morphology. Consequently the whisker aggregates may have been induced by the extrusion process.

In order to evaluate the influence of the extrusion process on the whiskers degradation, the whiskers length and diameter after extrusion were determined through TEM observations. Ramie whiskers were extracted from the extruded composite material by dissolving the composite in water. After dissolution of the PEO matrix, the cellulose whiskers were observed by TEM and compared to that directly obtained from the aqueous suspension (Fig. 7a, b). Uranyl acetate at a concentration of 2 wt% was used in order to emphasize the cellulose whiskers and create contrast.

As stressed in Fig. 7c, the effect of the extrusion process on the length of ramie whiskers is twofold: the extrusion greatly decreases the length of the main population, characterized by the peak position in the distribution, by a factor of about two, passing from about 200 to 120 nm. The second effect is the significant narrowing of the length distribution, showing that ramie whiskers are more monodisperse in length after extrusion. Such modifications in the length distribution can be properly attributed to a more efficient degradation of longer whiskers.

For this extruded composite, the cross section and length of whiskers were averaged over 300 measurements and they were found to be 5 ± 1 and 122 ± 45 nm, respectively, giving an aspect ratio around 24 ± 17. These values were compared to the initial average values of 7 ± 1, 200 ± 78 and 28 ± 12 nm, respectively. These results show that the extrusion process do not induce a significant change of the aspect ratio of the rod-like cellulosic nanoparticles. Indeed, even if individual variations of the cross section and length were reported, the impact on both is mostly equivalent.

Rheometry

The rheometrical characterization of PEO-based composites was performed through viscoelastic and creep measurements. For viscoelastic measurements, the linear regime was previously determined for each sample through a strain sweep test. At 90 °C, i.e. above the melting temperature, the critical strain, γ_c, marking

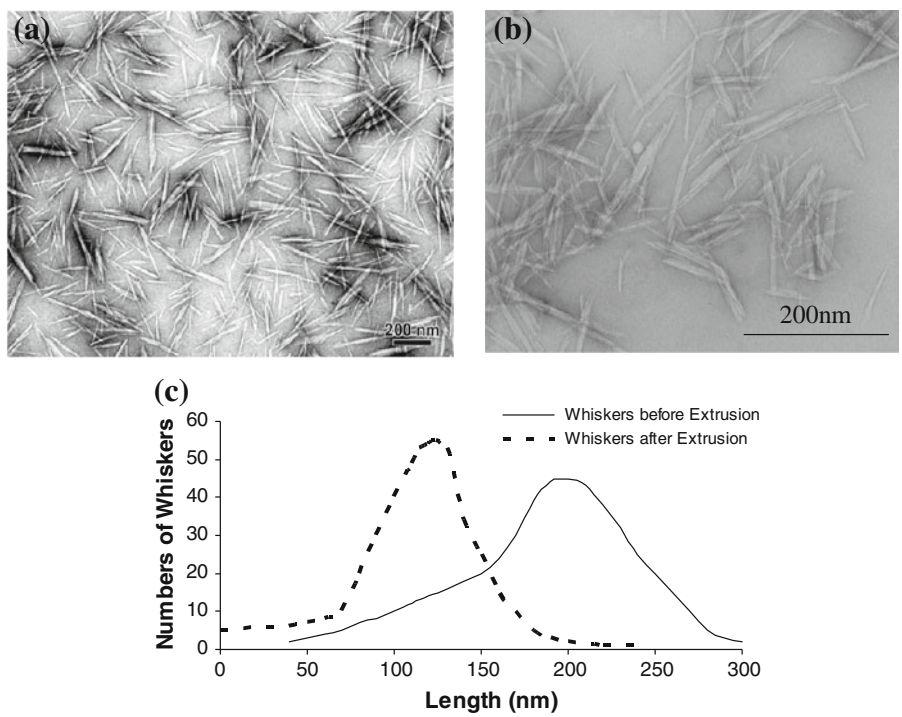

Fig. 7 Transmission electron micrographs (*TEM*) of **a** ramie whiskers suspension; **b** extruded and re-dispersed PEO nanocomposite films reinforced with 6 wt% of ramie whiskers; **c** their length distributions

the upper limit of the linear regime was about 0.5% for the cast/evaporated and extruded unfilled matrix while it decreased to 0.08% for the nanocomposites. The decrease of γ_c generally observed for encumbered systems, is due to the presence of ramie whiskers for nanocomposites.

Figure 8a, b show the evolution of both G' and G'' moduli as a function of the angular frequency for the neat PEO films and nanocomposites filled with 6 wt% of ramie whiskers, obtained by casting/evaporation and extrusion, respectively. The complex viscosity for all materials is presented in Fig. 8c.

Matrix behavior

Let's first examine the viscoelastic response of the matrix, processed by either casting/evaporation or extrusion.

In the case of cast/evaporated PEO films, the viscoelastic behavior is typical of melt polymers with the onset of a terminal zone at low frequency and the beginning of a rubbery plateau at high frequency, separated by a G'–G'' cross over at intermediate frequency. It has to be stressed that the frequency dependences of both moduli in the terminal zone, i.e. $G' \propto \omega^{0.8}$ and $G'' \propto \omega^{0.4}$, are quite lower than those expected for dense molecular systems with exponents of 2 and 1, respectively. Such lower frequency dependence of viscoelastic moduli in the terminal zone has been observed for PEO solutions and has been attributed to the presence of aggregates (Bossard et al. 2010). In the bulk, it could be the rheological signature of the presence of crystallites or spherulites in the amorphous phase.

The extruded PEO film (Fig. 8b) exhibits a viscoelastic behavior similar to the one of the cast/evaporated film with some quantitative differences: (1) the levels of both moduli, and consequently the complex viscosity, are lower for the extruded polymer than for the cast/evaporated one and (2) the terminal zone is shifted towards very low frequencies not explored and the G'–G'' cross-over is shifted towards higher frequencies. For the latter effect, it points out that the average relaxation time dynamics λ of PEO molecules, corresponding roughly to the inverse of the frequency of G'–G'' crossover, is speeded up after extrusion, passing from 2 to 0.2 s.

A decrease in the viscosity, associated with a speed up of the molecular dynamics and the broadening of the frequency region between the terminal zone and the G'–G'' cross-over after extrusion could be ascribed to a chain scission effect with a broadening in the polydispersity index of the polymer. Indeed, a similar effect has been observed for stirred PEO water solutions, and attributed mainly to the elongational flow induced by the dispersion procedure (Bossard

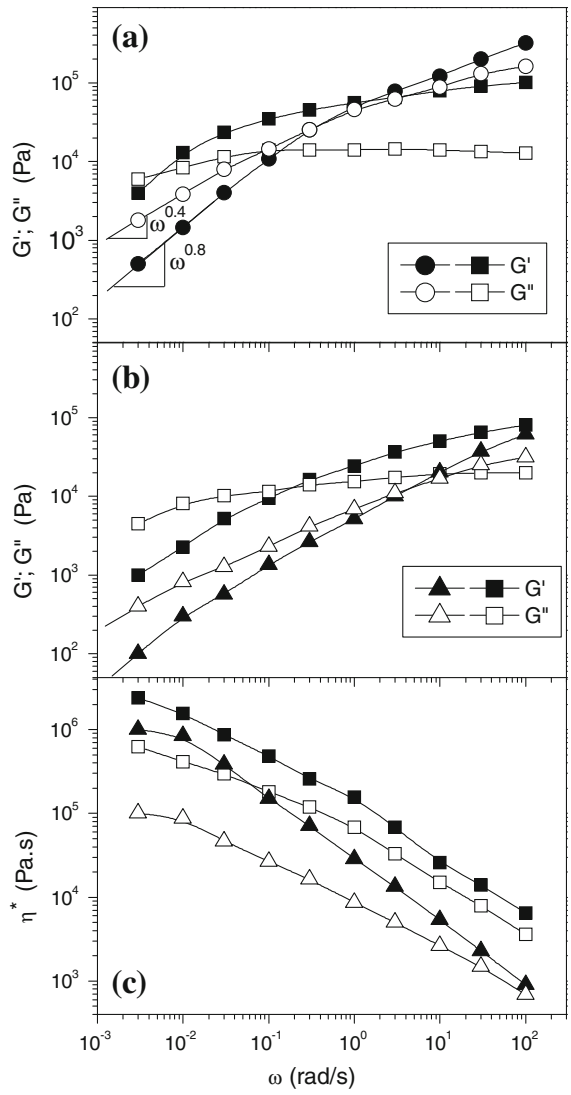

Fig. 8 Storage (G', *filled symbols*) and loss (G'', *open symbols*) moduli versus angular frequency at 90 °C for **a** the cast/evaporated unfilled PEO matrix (*circle*) and 6 wt% ramie whiskers reinforced nanocomposites (*square*), and **b** the extruded unfilled PEO matrix (*triangle*) and 6 wt% ramie whiskers reinforced nanocomposites (*square*). **c** Complex viscosity of the cast/evaporated (*square*) and extruded films (*triangle*) for matrices (*open symbols*) and composites (*filled symbols*) versus angular frequency

et al. 2010). Under extrusion that induces intense elongational flow, polymer chain scission is highly expected. To confirm this hypothesis, the average molecular weight of the extruded polymer was compared to the one obtained for the polymer processed by casting/evaporation using viscosity measurements. For this purpose, both films were dissolved and diluted at several concentrations in distilled water. The intrinsic viscosity $[\eta]$ was determined as the extrapolation to zero concentration of the reduced viscosity $\eta_{red.}$ defined in Eq. 4

$$\eta_{red.} = \frac{\eta_s - \eta_w}{C\eta_w} \quad (4)$$

with C, the solution concentration, η_s the zero-shear viscosity of polymer solutions and $\eta_w = 0.97$ mPas the Newtonian viscosity of water at 21 °C. Alternatively, $[\eta]$ can be obtained by fitting the so-called inherent viscosity, $\eta_{inh} = (\ln \eta_{rel})/c$ with the Kraemer equation

$$\frac{\ln \eta_{rel}}{c} = [\eta] - k_K[\eta]^2 c \quad (5)$$

where η_{rel} is the relative viscosity, $\eta_{rel} = \eta_0/\eta_w$ and k_K the Kraemer coefficient. The intrinsic viscosity is directly related to the molecular weight M by the Houwink-Mark-Sakurada equation (HMS),

$$[\eta] = KM^{\alpha} \quad (6)$$

where K and α are constants (Flory 1953). For PEO, HMS constants at 25 °C are equal to $K = 6.103 \times 10^{-3}$ cm^3 g^{-1} and $\alpha = 0.83$ (Khan 2006). The intrinsic viscosity of PEO solutions obtained from the cast/evaporated film is about $[\eta]_{cast-evap} = 900 \pm 150$ cm^{-3} g^{-1} while the one measured for the extruded film is $[\eta]_{cast-evap} = 520 \pm 80$ cm^{-3} g^{-1}, corresponding to an average molecular weight $M_{cast-evap} = (1.69 \pm 0.2) \times 10^6$ g/mol and $M_{extr.} = (8.7 \pm 1.6) \times 10^5$ g/mol, respectively. It thus appears that the decrease of the viscosity is effectively due to the significant mechanical degradation of PEO molecules after extrusion through chain scission.

Composite behavior

Let us consider and compare now the viscoelastic behavior of the two nanocomposites obtained either by casting/evaporation or extrusion. It can be seen in Fig. 8a, b that both materials exhibit viscoelastic moduli and a complex viscosity higher than that of their respective matrices, confirming the mechanical strengthen induced by the whiskers via whiskers/whiskers and whiskers/PEO interactions.

A similar behavior was reported by (Alvarez et al. 2004), with a saturation effect at higher fibers content. Indeed, strong interactions exist between PEO chains and cellulose. This effect is exacerbated because of the large cellulosic surface inherent to any nanoparticle. The PEO molecular dynamic is therefore locally restricted in the interfacial regions. This result is consistent with the pulse field NMR studies reported by (Azizi Samir et al. 2004b) for tunicin whiskers/PEO nanocomposites. These authors showed that the long relaxation time of PEO chains strongly decreased even with a low amount of whiskers owing to whiskers/PEO chains interactions.

However, some significant differences can be noticed between cast/evaporated and extruded nanocomposites. Viscoelastic moduli for the cast/evaporated nanocomposite in Fig. 8a are nearly frequency independent with $G' > G''$, except at very low frequency. This solid-like behavior would suggest the presence of a physical network, probably composed of ramie whiskers.

For the extruded nanocomposite, the viscoelastic moduli are frequency dependent and slightly lower than those of the cast/evaporated nanocomposite. After extrusion, the viscoelastic behavior is frequency depended thus suggesting the absence of a network, contrarily to what was observed for the cast/evaporated nanocomposite.

Consequently, it can be supposed that the extrusion prevents the formation of a network. In order to verify this hypothesis, creep measurements obtained for cast/evaporated and extruded nanocomposites submitted to the same stress have been compared in Fig. 9. The strain of the cast/evaporated nanocomposite reaches a plateau value beyond 1,500 s, corresponding to the mechanical response of a solid with a delayed elasticity while the one of the extruded nanocomposite gradually increases with time, which is characteristic of a fluid.

These results confirm the formation of a network for the cast/evaporated nanocomposite. In the case of the extruded nanocomposite, the whole set of rheological data suggests that whiskers do not form a network in the extruded film. However, the formation

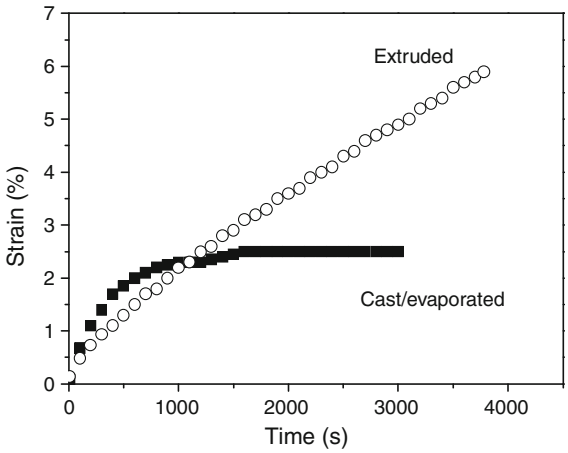

Fig. 9 Creep measurements ($\tau = 5$ μNm) for extruded (*open circle*) and cast/evaporated (*filled square*) composite reinforced with 6 wt% of ramie whiskers at 90 °C under inert atmosphere

of a weak network through low density H-bonds cannot be excluded.

Let us compare now the average relaxation time λ corresponding to the inverse of the frequency at the G'–G'' cross over.

In the case of PEO films, λ is divided by a factor of about 10 after extrusion. This speed up in the molecular dynamic has been attributed to PEO chain scission. For nanocomposites, the average relaxation time is divided by a factor of about 36, passing from 180 to 5 s.

As a consequence, differences in the relaxation dynamics of nanocomposites cannot be explained only by the modification of the matrix after extrusion but could be also due to the combined mechanical degradation and aggregation of whiskers, as stressed in Fig. 6 by SEM investigation and in Fig. 7a, b by TEM measurements. Indeed, break up of cellulose whiskers (Pathi and Jayaraman 2006) or natural fibers (Bengtsson et al. 2007) upon extrusion were already reported. (Alvarez et al. 2004) have shown that rheological properties of composite material are very sensitive to the diameter and aspect ratio of the fibers. Any process inducing a decrease of the fiber cross section and aspect ratio results in lower viscosity values.

Consequently, from a microstructural point of view, the general decrease of the rheological properties of the extruded nanocomposites compared to cast/evaporated ones may likely result from the contribution of four combined effects:

- The decrease of the rheological properties of the matrix through PEO chain scission induced by extrusion.
- The mechanical degradation of ramie whiskers during extrusion that reduces the ability of cellulosic fibers to connect each other.
- The whiskers aggregation induced by the extrusion process, which decreases the amount of whiskers available for the formation of the percolating network, as reported from SEM observation.
- And also the expected orientation effect of the extrusion process that prevents the formation of the percolation network.

Thermal characterization

Non-isothermal investigation

The thermal behavior of extruded samples was characterized using DSC. Results are reported in Table 3. The extruded PEO matrices obtained using either the PEO powder or pellets of freeze-dried PEO solution present similar thermal properties. Compared to the cast/evaporated neat sample (Table 3), the extruded neat samples display similar crystallization temperatures of about 51 °C, while both their melting temperatures and degrees of crystallinity decrease. A low value of the melting point is generally associated with a low value of lamellar thickness or/and a high value of the end interfacial free energy. These two parameters strongly depend on the crystallization process, i.e. melt crystallization or polymer precipitation in solution.

Table 3 Thermal characteristics of extruded PEO-based nanocomposites reinforced with ramie whiskers obtained from DSC curves: crystallization temperature (T_c), glass transition temperature (T_g), and degree of crystallinity expressed as a function of the matrix weight measured during the melting (χ_m)

Samples	T_g (°C)	T_c (°C)	T_m (°C)	χ_m^a
Extruded PEO powder	−55	52	49	0.76
Extruded freeze-dried PEO	−55	49	50	0.75
Extruded PEO + 6 wt% WR	−53	51	41	0.7

[a] $\chi_m = \frac{\Delta H_{m-PEO}}{\Delta H_m^0}$ where $\Delta H_m^0 = 210$ J g^{-1} is the heat of melting for 100% crystalline PEO

The significant differences in T_m and χ_m may be ascribed to (1) the processing technique itself, the spherulites size depending on the crystallization conditions, i.e. from the polymer melt or by polymer precipitation in solution, (2) the polymer chain scission during extrusion which may involve some polymer ramification and (3) the polymer orientation. Because of the lower degree of crystallinity, the glass transition can be observed at about −55 °C for extruded PEO matrices.

For the extruded samples, the T_m value significantly decreases, with a difference of 8 °C between filled and unfilled samples. This effect is much higher than the one observed for the cast/evaporated films for which no decrease of the melting point was observed with the incorporation of 6 wt% whiskers. The crystallization temperature was found to remain roughly constant.

Isothermal crystallization

In order to try to elucidate the crystallization process, isothermal crystallization kinetics were investigated. The growth rate of the PEO spherulites was determined for cast/evaporated and extruded matrix films using polarized optical microscopy. The sample was first melt at 100 °C for few minutes and cooled down to 50 or 55 °C. The linear growth rate is very sensitive to the imposed crystallization temperature. Indeed, due to the large difference in the behavior of the materials studied, two crystallization temperatures were investigated in order to crystallize the material in appropriate time.

For both matrices, cast/evaporated and extruded ones, the evolution of the PEO spherulites radius was monitored at 50 °C and results are reported in Fig. 10. The spherulites radii increase linearly with time for the two samples, which is generally observed for isothermal polymer crystallization. The kinetic of the radius growth is similar. However, a large difference exists, associated with the number of spherulites formed at a time t. The germ density, as observed during the optical investigation, for the extruded sample is high, thus the coalescence of spherulites occurs quickly and avoids the measurement of their radii beyond 50 s. As the germ density of the cast/evaporated matrix is much lower than for extruded one, the total crystallization is obtained after 300 s with a low density of large spherulites. The final spherulites radius sizes were estimated around 850 and 260 nm for the cast/evaporated and extruded matrices, respectively.

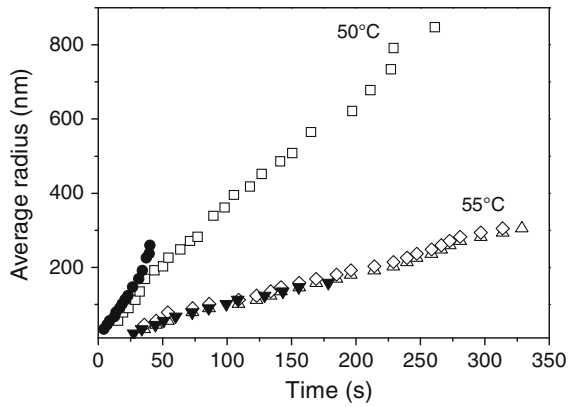

Fig. 10 Time dependence of the spherulites radius of extruded PEO matrix (*filled circle*) and cast/evaporated PEO matrix (*open square*) at 50 °C and extruded PEO matrix (*inverted triangle*) and extruded composite with 6 wt% of ramie whiskers (*open triangle*) and cast/evaporated PEO composite with 6 wt% of ramie whiskers (*diamond*) at 55 °C

The linear growth rate of spherulites for extruded PEO and nanocomposites has been studied at 55 °C. The increase of the crystallization temperature involves the presence of an induction time, necessary to obtain the first spherulites germ. The extruded composite sample exhibits the same linear growth rate of spherulites than the extruded PEO matrix. However, the setup fails to access the spherulites cross section for extruded PEO because it stops rapidly, after 180 s, due to the coalescence of the spherulites, as observed at 50 °C. The two composite samples exhibit the same kinetic, with the coalescence of the spherulites obtained after 300 s. For both extruded and cast/evaporated composites, the final spherulites radius was estimated around 330 nm.

Therefore, it appears that the elaboration process has an effect on the isothermal crystallization for the neat samples by a modification of the germ density. The extrusion process induces PEO degradation with a significant molecular weight decrease. This degradation may induce some defects, i.e. chain ramification which may increase the germ density as observed during optical measurements.

The incorporation of whiskers seems to vanish the influence of the processing technique on the linear growth rate of spherulites and their final radius. This may be related to the large influence of the presence

of the whiskers on the crystallization process. The incorporation of 6 wt% of whiskers has no effect on the linear growth rate, and thus doesn't modify the polymer chain mobility involved in the crystallization process. For cast/evaporated samples, the incorporation of 6 wt% whiskers involves an increase of the nucleation density.

Thermal degradation

The thermal degradation of the unfilled PEO and composite films was investigated under air. Composites and unfilled extruded films present a lower thermal stability than the cast/evaporated ones. Composites and unfilled extruded films have an onset degradation temperature of about 191 and 178 °C, respectively, compared to 205 and 191 °C for unfilled and composite cast/evaporated samples. The degradation process of PEO in the presence of oxygen is very complex (Costa et al. 1992). The lower degradation temperature of extruded films may be explained by the fact that during extrusion a significant mechanical degradation of PEO molecules through chain scission occurs. It may involve the formation of weaker links or end groups which are more sensitive to oxidative thermal degradation. Under helium, no effect of the processing technique was observed on thermal degradation and this invariance may be associated to the less aggressive atmosphere for PEO degradation.

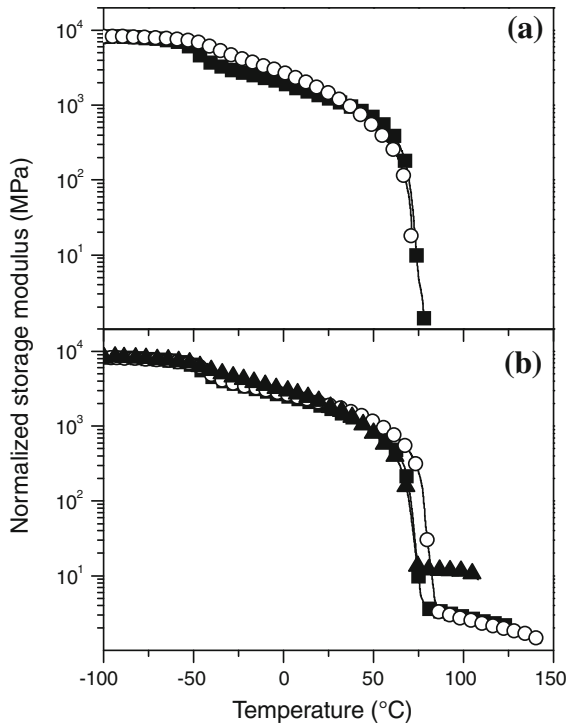

Fig. 11 Normalized storage modulus E' for **a** the neat cast/evaporated (*open circle*) and extruded (*filled square*) PEO matrices, and **b** nanocomposite films reinforced with 6 wt% of ramie whiskers obtained by casting-evaporation (*filled triangle*), strained in the extruded direction (*open circle*) and strained in the cross-sectional direction (*filled square*) as a function of temperature

Mechanical behavior

Dynamic mechanical measurements were performed for the extruded samples and compared to those obtained for the cast/evaporated films in Fig. 11. Here again, the storage tensile modulus E' at −100 °C was normalized at 8 GPa to minimize the influence of the error made for the determination of the sample dimensions. In accordance with its lower degree of crystallinity, as revealed by DSC measurements, the extruded PEO exhibits a higher modulus drop at T_g compared to the cast/evaporated matrix (Fig. 11a). Then, after the glass transition, the modulus continuously decreases because of the progressive melting of crystalline domains of PEO up to the melting point. The storage tensile modulus decrease near 65 °C is similar for the two matrices.

Dynamic mechanical measurements were performed for extruded nanocomposite films reinforced with 6 wt% of ramie whiskers (Fig. 11b) for samples cut in the extrusion direction and in the cross-sectional one. (Kvien and Oksman 2007) have shown that using a strong magnetic field, which induces a cellulose whiskers orientation, the nanocomposite film modulus in the cross-sectional direction is higher than that in the extrusion one. For extruded PEO nanocomposites, the curves obtained for the sample cut in the two directions are overlapped indicating that no orientation of the whiskers occurs during extrusion. Thus one hypothesis developed in regard to rheological measurements to explain the decrease in rheological properties is suppressed by mechanical investigation.

The experimental modulus of the extruded composite was found around $E'_{exp} = 2$ MPa, compared to 12 MPa for the cast/evaporated nanocomposite film reinforced with 6 wt% of ramie whiskers. The high temperature storage modulus of the filled extruded

membrane is therefore notably lower than the one of the filled cast/evaporated membrane.

Even if the whisker aspect ratio was slightly reduced as discussed previously, 24 instead of 28, the amount of whiskers in the extruded membrane, i.e. 6 wt% (4.86 vol%), is theoretically sufficient to obtain a percolating network because the critical volume fraction of the filler at the percolation threshold calculated using an aspect ratio of 24 is $\upsilon_{Rc} = 2.9$ vol%. Nevertheless, the presence of whisker aggregates in the filled extruded membrane, observed by MEB investigation, decreases notably the amount of whiskers available to form a network. Moreover, in cast/evaporated films, the kinetic of the film formation and the viscosity of the medium, at least at the beginning of the process are low. These two parameters give time to the formation of a whiskers network in cast/evaporated membranes.

On the contrary, during the extrusion process, a high viscosity value for the matrix, a fast process kinetic and mechanical stress could restrict the number of H-bonds formed during whiskers network formation. Thus a weak network or in the limit case no network may be formed.

At high temperature, instead of the E'_{exp} plateau, obtained in the case of cast/evaporated films characterized by DMA measurement (Fig. 11), a straight line with a slope of about -0.03 MPa $°C^{-1}$ for extruded composites is observed. This behavior may be associated with the absence of network or the presence of a weak network.

As mentioned previously, the invariance of E'_{exp} with temperature for cast/evaporated composites was attributed to a high density of H-bonds. Thus the decrease of E'_{exp} versus temperature for extruded sample is in agreement with a low density H-bonded network. Indeed, as the H-bonded strength decreases with temperature, a low density H-bonded network may have the same behavior.

Conclusions

Nanocomposite films based on PEO polymer as the matrix and cellulose whiskers extracted from ramie plant as the reinforcing phase were obtained by casting/evaporation and extrusion processes. Microscopic observations show some whiskers aggregations and a small decrease of the whiskers aspect ratio for extruded sample, but for both processes employed, films display homogeneous surfaces.

The rheological behavior for cast/evaporated films shows that viscoelastic and creep measurements have a solid-like behavior, according to mechanical measurement exhibiting a spectacular reinforcement after melting temperature. These high mechanical performances for the casting/evaporation process are ascribed to the formation of a rigid cellulosic network.

For the extruded composites, the rheological behavior through the viscoelastic and creep measurements shows a liquid-like behavior. This stresses a weak reinforcement behavior obtained for extruded composites. This weak mechanical reinforcement after the PEO melting temperature leads us to conclude that the extrusion process prevents the formation of a strong whiskers network for the whiskers content used, contrary to evaporated films. One possibility to improve this reinforcement, taking into account the aggregation and the decrease of the aspect ratio of whiskers during the extrusion process, is to increase the filler content. Even if the extrusion process requires a higher whisker content to obtain the same result compared to the casting/evaporation process, it is worth noting that the former is much less time consuming.

Acknowledgments The authors thank Dr. Youssef Habibi for his support in the whiskers preparation and Mme Denise Foscallo for TGA measurements.

References

Alvarez V, Terenzi A, Kenny JM, Vazquez A (2004) Melt rheological behavior of starch-based matrix composites reinforced with short sisal fibers. Polym Eng Sci 44: 1907–1914

Anglés MN, Dufresne A (2000) Plasticized/tunicin whiskers nanocomposites materials. 1. Structural analysis. Macromolecules 33:8344–8353

Azizi Samir MAS, Alloin F, Sanchez J-Y, Dufresne A (2004a) Cellulose nanocrystals reinforced poly(oxyethylene). Polymer 45:4149–4157

Azizi Samir MAS, Alloin F, Gorecki W, Sanchez J-Y, Dufresne A (2004b) Nanocomposite polymer electrolytes based on poly(oxyethylene) and cellulose nanocrystals. J Phys Chem B 108:10845–10852

Azizi Samir MAS, Alloin F, Dufresne A (2005a) A review of recent research into cellulosic whiskers, their properties and their application in nanocomposite field. Biomacromolecules 6:612–626

Azizi Samir MAS, Chazeau L, Alloin F, Cavaillé J-Y, Dufresne A, Sanchez J-Y (2005b) POE based nanocomposite polymer electrolytes reinforced with cellulose whiskers. Electrochim Acta 50:3897–3903

Bengtsson M, Le Baillif M, Oksman K (2007) Extrusion and mechanical properties of highly filled cellulose fiber-polypropylene composites. Compos Part A 38:1922–1931

Bondeson D, Oksman K (2007) Whisker nanocomposites modified by polyvinyl alcohol. Compos Part A 38: 2486–2492

Bossard F, El Kissi N, D'Aprea A, Alloin F, Sanchez J-Y, Dufresne A (2010) Influence of turbulent flow on rheological properties of aqueous solutions of high molecular weight PEO. Rheol Acta 49:529–540

Bras J, Viet D, Bruzzese C, Dufresne A (2010) Correlation between stiffness of sheets prepared from cellulose whiskers and nanoparticles dimensions. Carbohydr Polym (in press). doi:10.1016/j.carbpol.2010.11.022

Broido A (1969) A simple, sensitive graphical method of treating thermogravimetric analysis data. J Polym Sci Part A-2 7:1761–1773

Cameron GG, Ingram MD, Qureshi MY, Gearing HM, Costa L, Camino G (1989) The thermal degradation of poly(ethylene oxide) and its complex with NaCNS. Eur Polym J 25:779–784

Chauvin C, Ollivrin X, Alloin F, Le Nest J-F, Sanchez J-Y (2005) Lithium salts based on oligoether sulfate esters. Electrochim Acta 50:3843–3852

Chauvin C, Alloin F, Iojoiu C, Sanchez J-Y (2006) New polymer electrolytes based on ether sulfate anions for lithium polymer batteries. Part I: multifunctional ionomers: conductivity and electrochemical stability. Electrochim Acta 51:5876–5884

Costa L, Gad AM, Camino G, Cameron GG, Qureshi MY (1992) Thermal and thermooxidative degradation of poly(ethylene oxide)-metal salt complexes. Macromolecules 25:5512–5518

De Gennes PG (ed) (1979) Scaling concepts in polymer physics. Cornell University Press, Ithaca, p 223

De Menezes AJ, Siqueira G, Curvelo AAS, Dufresne A (2009) Extrusion and characterization of functionalized cellulose whisker reinforced polyethylene nanocomposites. Polymer 50:4552–4563

Dufresne A, Cavaillé J-Y, Helbert W (1997) Thermoplastic nanocomposites filled with wheat straw cellulose whiskers. Part II: effect of processing and modeling. Polym Compos 18:198–210

Favier V, Canova GR, Cavaillé J-Y, Chanzy H, Dufresne A, Gauthier C (1995) Nanocomposites from latex and cellulose whiskers. Polym Adv Technol 6:351–355

Favier V, Canova GR, Shrivastava SC, Cavaillé J-Y (1997) Mechanical percolation in cellulose whisker nanocomposites. Polym Eng Sci 37:1732–1739

Flory PI (ed) (1953) Principles of polymer chemistry. Cornell University Press, Ithaca, p 495

Grassie N, Mendoza GAP (1985) Thermal degradation of polyether-urethanes: part 2—influence of the fire retardant, ammonium polyphosphate, on the thermal degradation of poly(ethylene glycol). Polym Degrad Stab 10:43–54

Guo YQ, Liang XH (1999) The miscibility of cellulose-polyethylene glycol blends. J Macromol Sci B 38:439–447

Habibi Y, Dufresne A (2008) Highly filled bionanocomposites from functionalized polysaccharides nanocrystals. Biomacromolecule 9:1974–1980

Habibi Y, Foulon L, Aguie-Beghin V, Molinari M, Douillard RJ (2007) Langmuir-Blodgett films of cellulose nanocrystals: preparation and characterization. Colloid Interface Sci 316:388–397

Julien S, Chornet E, Overend RP (1993) Influence of acid pretreatment (H_2SO_4, HCl, HNO_3) on reaction selectivity in the vacuum pyrolysis of cellulose. J Anal Appl Pyrolysis 27:25–43

Khan MS (2006) Aggregate formation in poly(ethylene oxide) solutions. J Appl Polym Sci 102:2578–2583

Kim DY, Nishiyama Y, Wada M, Kuga S (2001) High-yield carbonization of cellulose by sulfuric acid impregnation. Cellulose 8:29–33

Kvien S, Oksman K (2007) Orientation of cellulose nanowhiskers in polyvinyl alcohol (PVA). Appl Phys A 87:641–643

Oksman K, Mathew AP, Bondeson D, Kvien I (2006) Manufacturing process of cellulose whiskers. Compos Sci Technol 66:2776–2784

Panaitescu DM, Vuluga DM, Paven H, Iorga MD, Ghiurea M, Matasaru I, Nechita P (2008) Properties of polymer composites with cellulose microfibrils. Mol Cryst Liq Cryst 484:86–98

Parks EJ (1971) Thermal analysis of modified cellulose. J Tappi 54:537–544

Pathi S, Jayaraman K (2006) Effects of extrusion on fiber length in sisal fiber-reinforced polypropylene composites. Int J Mod Phys B 20:4607–4612

Roman M, Winter WT (2004) Nanocomposites of cellulose acetate butyrate reinforced with cellulose nanocrystals. Biomacromolecules 5:1671–1677

Scheirs J, Camino G, Tumiatti W (2001) Overview of water evolution during the thermal degradation of cellulose. Eur Polym J 37:933–942

Takayanagi M, Uemura S, Minami S (1964) Application of equivalent model method to dynamic rheo-optical properties of a crystalline polymer. J Polym Sci Part C 5: 113–122

Tang WK, Neill WK (1964) Effect of flame retardants on pyrolysis and combustion of α-cellulose. J Polym Sci Part C 6:65–79